Transition from weak to strong measurements by nonlinear quantum feedback control

Jing Zhang,[1,2,3,*] Yu-xi Liu,[2,4] Re-Bing Wu,[1,2] Chun-Wen Li,[1,2] and Tzyh-Jong Tarn[2,5]

[1]*Department of Automation, Tsinghua University, Beijing 100084, People's Republic of China*

[2]*Center for Quantum Information Science and Technology, Tsinghua National Laboratory for Information Science and Technology, Beijing 100084, People's Republic of China*

[3]*Department of Physics and National Center for Theoretical Sciences, National Cheng Kung University, Tainan 70101, Taiwan*

[4]*Institute of Microelectronics, Tsinghua University, Beijing 100084, People's Republic of China*

[5]*Department of Electrical and Systems Engineering, Washington University, St. Louis, Missouri 63130, USA*

(Received 26 June 2009; revised manuscript received 7 May 2010; published 6 August 2010)

We find that feedback control may induce "pseudo"-nonlinear dynamics in a damped harmonic oscillator, whose centroid trajectory in the phase space behaves like a classical nonlinear system. Thus, similar to nonlinear amplifiers (e.g., rf-driven Josephson junctions), feedback control on the harmonic oscillator can induce nonlinear bifurcation, which can be used to amplify small signals and further to measure quantum states of qubits. Using the cavity QED and the circuit QED systems as examples, we show how to apply our method to measuring the states of two-level atoms and superconducting charge qubits.

DOI: 10.1103/PhysRevA.82.022101 PACS number(s): 03.65.Ta, 03.65.Sq, 05.45.−a, 85.25.−j

I. INTRODUCTION

Quantum feedback control [1] is one of the central parts of quantum control theory and applications [2–6] owing to its potential ability to improve the stability and robustness of the system. Besides the extensive theoretical studies [7–11], recent rapid developments on sensitive measurements and manipulation techniques in atom-optical [12–14] and solid-state systems [15] have made it possible to implement quantum feedback control in laboratories.

In atom-optical systems, atomic ensembles are put in high-Q optical cavities, so that the information of the states of the atomic ensembles can be extracted by the probe lights transmitted through the optical cavities. Photocurrents induced by the probe lights are processed by field programmable gate arrays to generate real-time control signals, which can be fed back to design the electromagnetic fields imposed on the atomic ensembles [12]. Possible applications of quantum feedback control in such systems include state stabilization [16], entanglement production [17], spin squeezing [18], and state discrimination [13,14]. Similar studies can be found in solid-state systems [19], for example, the superconducting circuit QED systems, in which quantum feedback control has been proposed to cool and squeeze the motion of a nanomechanical resonator [20–23]. In these studies, the position of the nanomechanical resonator can be measured by a single electron transistor [21] or a rf-superconducting quantum interference device [22,24,25].

Most existing theoretical studies on quantum feedback control are concentrated on linear quantum systems; that is, the dynamical equations of the system are linear in the Heisenberg picture and the feedback controls are linear functions of the system states, which can often be reduced to standard classical control problems, for example, the linear quadratic Gaussian control problem [9,10]. However, essential differences arise when we study nonlinear quantum systems: (i) linear quantum systems possess evenly spaced discrete energy spectra, while the distributions of energy levels in nonlinear systems are uneven or continuous; (ii) linear quantum system starting from a Gaussian state always stays in a Gaussian state during the evolution, while nonlinear quantum dynamics generally distorts the wave packet. Moreover, the presence of the relaxation and dephasing effects in nonlinear quantum systems may give rise to inherent phenomena in nonlinear classical systems, for example, chaos [26] and bifurcation [27]. These dissipation-induced nonlinear effects [26,27] have various applications in laboratories. For example, nonlinear dynamical bifurcation of a rf-driven Josephson junction is used to amplify small signals [28] and further applied to the readouts of the superconducting qubit states in experiments [28,29].

Here we propose a method to mimic nonlinear dynamics using a harmonic oscillator with the feedback control. Such a proposal can be widely applied, especially in circumstances where a nonlinear amplifier like the rf-driven Josephson junction is not achievable. It should be noticed that the manipulation of nonlinear effects via feedback has been widely studied in classical systems [30]. However, to what extent can we apply this to quantum systems? In particular, an extensively discussed question is whether the nonlinear effects [31] can be produced in linear quantum systems by quantum feedback control. Here we address this question by examining a damped harmonic oscillator driven by a nonlinear feedback control and show that using this "pseudo"-nonlinear amplifier can read out quantum states of qubits.

Our proposal is motivated by the recent developments for the quantum-state readouts in superconducting quantum circuits via a nonlinear amplifier [28] and the quantum information processing using the cavity QED effect (e.g., in atom-optical systems, cavity quantum-dot systems, and the systems for the interaction between superconducting qubits and the transmission line resonator). In contrast to the measurement of the quantum states using a nonlinear amplifier (e.g., reading out the states of a superconducting qubit using a rf-driven Josephson junction [28]), one merit for our study is that in the long-time limit we can analytically analyze the dynamics of the qubit-oscillator system even in the "nonlinear" regime, which makes it possible to see how to control the

*jing-zhang@mail.tsinghua.edu.cn

rate of the information extraction so as to balance between the measurement sensitivity and the measurement-induced disturbance in the bifurcation readout regime. Our study can be applied to the measurement of the states of an atom inside a cavity, quantum dots interacting with single-mode cavity field, or superconducting qubits in the circuit QED systems. Without loss of generality, in what follows we choose the atom-cavity system and the circuit QED system as examples to demonstrate our method, because these two kinds of systems are more experimentally controllable and developed very quickly in recent years. Thus, our proposal might be more possible to be demonstrated in these systems.

The article is organized as follows: In Sec. II, we present our feedback-control proposal using a general model in which a damped harmonic oscillator is measured by a homodyne detection and then driven by the output field of the feedback-control loop. The model of a system in which a harmonic oscillator is dispersively coupled to a qubit and driven by an outer feedback-control circuit is discussed in Sec. III. Also, the analysis of the bifurcation-induced qubit readout by a harmonic oscillator with pseudo-nonlinear dynamics is given in this section. The applications to the atom-cavity systems and the circuit QED systems are shown in Sec. IV, and the conclusions and discussions are given in Sec. V.

II. CONTROLLED DAMPED HARMONIC OSCILLATOR

Consider a damped harmonic oscillator with an angular frequency ω and a damping rate γ, which is driven by a control signal u_t. Let us assume that the decay of the harmonic oscillator can be detected by a homodyne measurement with efficiency η. Under the weak measurement assumption [32], the dynamics of the harmonic oscillator with the state ρ and the measurement output dy for measuring the position operator x can be described by the stochastic equations [8–12]

$$d\rho = -\frac{i}{\hbar}[H,\rho]dt + \gamma\mathcal{D}[a]\rho dt + \sqrt{\eta\gamma}\mathcal{H}[a]\rho dW, \quad (1)$$

$$dy = \langle x\rangle dt + \frac{1}{\sqrt{2\eta\gamma}}dW, \quad (2)$$

where $\langle x\rangle = \mathrm{tr}(x\rho)$ is the average of the position operator x; a and $a^\dagger$ are the annihilation and creation operators, respectively, of the driven harmonic oscillator whose Hamiltonian is

$$H = \hbar\omega a^\dagger a + \hbar u_t x. \quad (3)$$

The term $\hbar u_t x$ represents the interaction between the harmonic oscillator and a time-dependent classical control field characterized by u_t. The superoperators $\mathcal{D}[a]\rho$ and $\mathcal{H}[a]\rho$ are defined by

$$\mathcal{D}[a]\rho = a\rho a^\dagger - \tfrac{1}{2}(a^\dagger a\rho + \rho a^\dagger a),$$
$$\mathcal{H}[a]\rho = a\rho + \rho a^\dagger - \mathrm{tr}(a\rho + \rho a^\dagger)\rho.$$

The measurement is performed over the position operator

$$x = \frac{1}{\sqrt{2}}(a + a^\dagger),$$

whose conjugate momentum operator is

$$p = \frac{i}{\sqrt{2}}(a^\dagger - a).$$

dW is a measurement-induced Wiener noise satisfying

$$E(dW) = 0, \quad (dW)^2 = dt,$$

with $E(\cdot)$ representing the ensemble average over the stochastic noise.

As shown in Eq. (2), dW represents the measurement-induced noise in the measurement output of the homodyne detection. To reduce the influence of the noise in the feedback-control design, we take the time average

$$Y_t = \frac{1}{t}\int_0^t \left(\langle x\rangle d\tau + \frac{1}{\sqrt{2\eta\gamma}}dW\right) = \frac{1}{t}\int_0^t dy \quad (4)$$

of the output signal, where $t \gg 1/\gamma$, as an estimation of the position x. Taking the long-time average of the stochastic signals is an effective filtering strategy for extracting stationary signals from the background noises, and the time-average signal, for example, Y_t in Eq. (4), can be further used to design feedback control. Such a control design has been used in the literature to prepare desired quantum states (see, e.g., Ref. [33] for the Dicke state preparation).

With these considerations, we apply the nonlinear feedback control

$$u_t = f(Y_t) = -k_1 Y_t + k_3 Y_t^3 - k_0 \quad (5)$$

to the original system (1) described by the Hamiltonian in Eq. (3), where the positive numbers k_0, k_1, and k_3 are the control parameters. In the following discussions, the control parameters k_1 will be chosen such that $k_1 > \gamma$.

The nonlinear feedback control given by Eq. (5) induces a pitchfork static bifurcation by varying the bifurcation parameter ω near the bifurcation point:

$$\omega^* = \tfrac{1}{2}\left(k_1 - \sqrt{k_1^2 - \gamma^2}\right). \quad (6)$$

In fact, if the initial state of the harmonic oscillator is a Gaussian state ρ_0 with

$$\langle x\rangle_{\rho_0} = 0, \quad \langle p\rangle_{\rho_0} = 0,$$
$$\langle x^2\rangle_{\rho_0} - \langle x\rangle_{\rho_0}^2 = V_{x_0},$$
$$\langle p^2\rangle_{\rho_0} - \langle p\rangle_{\rho_0}^2 = V_{p_0},$$
$$\tfrac{1}{2}\langle px + xp\rangle_{\rho_0} - \langle x\rangle_{\rho_0}\langle p\rangle_{\rho_0} = C_{x_0p_0}, \quad (7)$$

and if the bifurcation parameter ω is below ω^*, then the state of the harmonic oscillator given by Eq. (1) converges to the following stationary coherent state:

$$|\alpha_0^\infty\rangle = \left|\frac{1}{\sqrt{2}}\left(x_0^\infty + ip_0^\infty\right)\right\rangle, \quad (8)$$

where

$$x_0^\infty = \frac{2\omega}{\gamma}p_0^\infty = k_0\frac{\omega}{\omega^2 - k_1\omega + \gamma^2/4}. \quad (9)$$

However, if the bifurcation parameter ω exceeds ω^*, the original stationary state given by Eq. (8) becomes unstable, and two new branches of stationary coherent states appear:

$$|\alpha_{1,2}^{\infty}\rangle = \left|\frac{1}{\sqrt{2}}\left(x_{1,2}^{\infty} + ip_{1,2}^{\infty}\right)\right\rangle, \tag{10}$$

where

$$x_{1,2}^{\infty} = \frac{2\omega}{\gamma} p_{1,2}^{\infty} = \pm\sqrt{\frac{-\omega^2 + k_1\omega - \gamma^2/4}{k_3\omega}}. \tag{11}$$

The analyses of the preceding results can be found in Appendix A. It can be verified that $|\alpha_{1,2}^{\infty}\rangle$ are far away from the original stationary state $|\alpha_0^{\infty}\rangle$ if the parameters k_0 and k_3 are small enough such that

$$k_0, k_3 \ll \left|\frac{\omega^2 - k_1\omega + \gamma^2/4}{\omega}\right|. \tag{12}$$

To give more insights about the preceding results, we see that Y_t and $\bar{x} = E(\langle x\rangle)$ coincide together in the long-time limit [see Eqs. (A5) and (A8) in Appendix A], and thus $(x_0^{\infty}, p_0^{\infty})^T$ and $(x_{1,2}^{\infty}, p_{1,2}^{\infty})^T$ are just the stationary states of the dynamical equation:

$$\begin{aligned} \dot{x} &= -\frac{\gamma}{2}x + \omega p, \\ \dot{p} &= -(\omega - k_1)x - k_3x^3 - \frac{\gamma}{2}p + k_0. \end{aligned} \tag{13}$$

In fact, it can be verified that the preceding equation has one stable equilibrium $(x_0^{\infty}, p_0^{\infty})^T$ when $\omega < \omega^*$ and two stable equilibria $(x_{1,2}^{\infty}, p_{1,2}^{\infty})^T$ when $\omega > \omega^*$, which coincides with the results given in Eqs. (9) and (11).

It should be pointed out that the feedback control presented here is different from the Markovian feedback [8] and Bayes feedback controls [9], in which the white-noise term dW in Eq. (2) is looked at as an innovation information term obtained by measuring a single system and used to update the feedback control. In contrast, our proposal is quite similar to a feedback-control proposal based on the measurement over an ensemble of harmonic oscillators. In fact, the measurement output given by Eq. (2) can be re-expressed as

$$I(t) = \langle x\rangle + \frac{1}{\sqrt{2\eta\gamma}}\xi(t),$$

where $\xi(t)$ satisfies

$$E(\xi(t)) = 0, \quad \xi(t)\xi(t') = \delta(t - t').$$

Then we take the average of the measurement output over the quantum ensemble to obtain $\bar{x} = E(I(t)) = E(\langle x\rangle)$, which can be further used to design feedback control $u_t = u(\bar{x})$, and the same feedback control is imposed on each system in the quantum ensemble. Here, we have only a single system, and thus, different from the preceding ensemble feedback-control proposal, we take the time-averaged Y_t given in Eq. (4) to replace the ensemble average $\bar{x}$. Since the system state given by Eq. (1) tends to a stationary state given by Eq. (8) or (10), Y_t and $\bar{x}$ coincide together in the long-time limit from the ergodic theory [34] [see Eqs. (A5) and (A8) in Appendix A]. Thus, our feedback-control proposal is similar to the ensemble nonlinear feedback control in the long-time limit. Compared with the existing feedback-control proposals, for example, the Bayes feedback, our method is more robust to the uncertainty of the initial state. In fact, the same stationary states given by Eqs. (8) and (10) can be obtained if the initial state of the system deviates slightly from the Gaussian state given by Eq. (7).

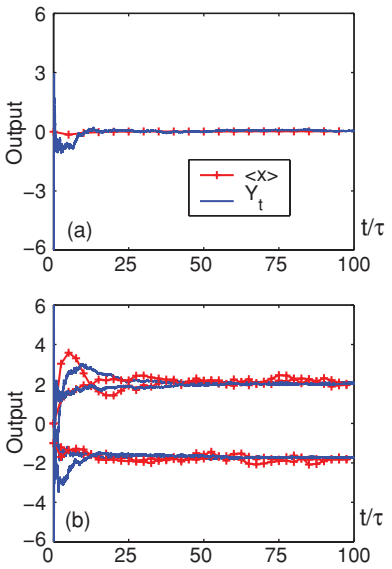

FIG. 1. (Color online) Stochastic pitchfork bifurcation given by Eqs. (1), (2), and (5) with (a) $\omega = 3.5$ MHz and (b) $\omega = 65$ MHz. The parameter $\tau = 2$ ns is the normalization time scale. The red curves with plus signs [one curve in (a) and four curves in (b)] represent the stochastic trajectories $\langle x\rangle_t$, and the blue solid curves [one curve in (a) and four curves in (b)] denote the time-averaged trajectories Y_t given by Eq. (4).

To show the validity of our feedback-control proposal, let us show some numerical examples. By setting the system parameters as $\gamma = 250$ MHz, $k_0 = 50$ MHz, $k_1 = 500$ MHz, $k_3 = 50$ MHz, $\omega = 3.5$ MHz, $x_0 = p_0 = 0$, $V_{x_0} = V_{p_0} = 1$, and $C_{x_0p_0} = 0$, the simulation results in Fig. 1(a) show that both $\langle x\rangle$ and Y_t converge to a stationary state $x_0^{\infty} = 0.0126 \approx 0$ given by Eq. (9). However, if we tune the oscillating frequency of the harmonic oscillator such that $\omega = 65$ MHz, the stochastic trajectories of $\langle x\rangle$ and Y_t are separated into two branches which tend to two different stationary states $x_{1,2}^{\infty} = \pm 1.95$ given by Eq. (11). The preceding simulation results coincide with the theoretical analysis.

As analyzed in Appendix A, the first-order quadratures $\langle x\rangle$ and $\langle p\rangle$ of the controlled system evolve nonlinearly in the long-time limit, while the higher-order quadratures approach those of the linear quantum systems which preserve the Gaussian properties of the states. Therefore, the nonlinear dynamics induced by the proposed quantum feedback control is "semiclassical" in some sense (see the simplified diagram of the feedback control circuit in Fig. 2), in contrast to the dynamics of the system governed by a fully quantum nonlinear Hamiltonian (about x and p) such as

$$H_{\rm nl} = \tfrac{1}{2}p^2 + \tfrac{1}{2}\omega^2x^2 - kx^4, \tag{14}$$

in which the Gaussian wave packets are distorted. Here the subscript "nl" means that the Hamiltonian contains higher-order nonlinear terms. In our feedback-control

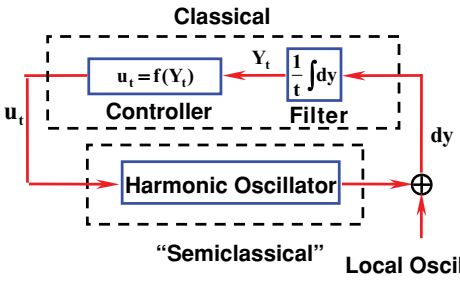

FIG. 2. (Color online) Schematic diagram of the feedback control circuit. The harmonic oscillator is measured by a homodyne detection, and the output signal of the homodyne measurement is fed into a classical control circuit which is composed of a integral filter and a controller. The output signal of the control circuit is further fed back to drive the harmonic oscillator, and this feedback control signal may induce nonlinear dynamics of the harmonic oscillator.

proposal, we introduce nonlinear terms such as $\langle x\rangle^3$ to the dynamical equation of the system in comparison to the terms $\langle x^3\rangle$ introduced by the nonlinear Hamiltonian $H_{\rm nl}$ in Eq. (14). Thus, under the nonlinear Hamiltonian $H_{\rm nl}$, the equations of the first-order quadratures $\langle x\rangle$ and $\langle p\rangle$ and the second-order quadratures V_x, V_p, and C_{xp} are not closed since higher-order quadratures such as $\langle x^3\rangle$ are involved. However, in our proposal, the equations of $\langle x\rangle$, $\langle p\rangle$ and V_x, V_p, C_{xp} are closed and decoupled just like a linear harmonic oscillator if the initial state of the harmonic oscillator is a Gaussian state (see the analysis in the Appendix A), whose stationary solution can be analytically solved. For this reason, we call this feedback-control-induced nonlinear dynamics "pseudo"-nonlinear dynamics. As shown in what follows, interesting phenomena can be observed when such a pseudo-nonlinear system is coupled to another quantum system. That is, similar to the nonlinear amplifier using the nonlinear dynamical bifurcation (e.g., rf-driven Josephson junctions [28]), the harmonic oscillator with feedback control can be used to amplify small signals and furthermore to read out the qubit states.

III. MEASUREMENTS ON QUBIT STATES USING CONTROLLED HARMONIC OSCILLATOR

A. Qubit-oscillator coupling

To demonstrate how we can use the pseudo-nonlinear harmonic oscillator produced by feedback control to measure qubit states, let us consider a coupled qubit-oscillator system driven by a classical field with angular frequency ω_d. The Hamiltonian of this system can be expressed as

$$H = \frac{\hbar\omega_q}{2}\sigma_z + \hbar\omega_o a^\dagger a + \hbar g(a^\dagger\sigma_- + a\sigma_+) + \hbar u_t\frac{1}{\sqrt{2}}(a^\dagger e^{-i\omega_d t} + a e^{i\omega_d t}), \quad (15)$$

where ω_q and ω_o are the angular frequencies of the qubit and the harmonic oscillator; σ_z and $\sigma_\pm$ are the z-axis Pauli operator and ladder operators of the qubit; a and $a^\dagger$ are the annihilation and creation operators, respectively, of the harmonic oscillator; g is the qubit-oscillator coupling strength; and u_t is the coupling constant between the driving field and the harmonic oscillator.

In the dispersive regime, that is, $|\Delta_{qo}| = |\omega_q - \omega_o| \gg |g|$, we can apply the unitary transformation

$$U = \exp\left[\frac{g}{\Delta_{qo}}(a\sigma^\dagger - a^\dagger\sigma_-)\right]$$

to the Hamiltonian H in Eq. (15); then we have an effective Hamiltonian,

$$\tilde{H} = UHU^\dagger \approx \frac{\hbar(\omega_q+\chi)}{2}\sigma_z + \hbar\omega_o a^\dagger a + \hbar\chi a^\dagger a\sigma_z + \hbar u_t\frac{1}{\sqrt{2}}(a^\dagger e^{-i\omega_d t} + a e^{i\omega_d t}), \quad (16)$$

where $\chi = g^2/\Delta_{qo}$ is the effective coupling strength between the qubit and the harmonic oscillator.

Furthermore, the Hamiltonian $\tilde{H}$ can be rewritten in the rotating reference frame under the unitary transformation

$$U_{\rm rot} = \exp[i(\omega_d t)a^\dagger a];$$

thus, we can obtain the following effective Hamiltonian:

$$H_{\rm eff} = U_{\rm rot}\tilde{H}U_{\rm rot}^\dagger + i\dot{U}_{\rm rot}U_{\rm rot}^\dagger = \frac{\hbar\omega_q}{2}\sigma_z + \hbar\Delta_{od}a^\dagger a + \hbar\chi a^\dagger a\sigma_z + \hbar u_t x, \quad (17)$$

where $\Delta_{od} = \omega_o - \omega_d$ is the angular frequency detuning between the harmonic oscillator and the driving field; and $x = (a + a^\dagger)/\sqrt{2}$ is the position operator of the harmonic oscillator. Here the frequency shift of the qubit caused by the harmonic oscillator has been neglected under the assumption that $\omega_q \gg \chi$, which is usually valid in atom-optical systems and superconducting circuits.

If we expand the Hamiltonian in Eq. (16) to $(g/\Delta_{qo})^3$ terms, we can obtain the following effective nonlinear Hamiltonain:

$$\tilde{H}_{\rm eff} = \frac{\hbar}{2}\left(\omega_q + \frac{g^2}{\Delta_{qo}} + \frac{g^4}{2\Delta_{qo}^3}\right)\sigma_z + \hbar\Delta_{od}a^\dagger a + \hbar\frac{g^2}{\Delta_{qo}}a^\dagger a\sigma_z - \hbar\frac{g^4}{\Delta_{qo}^3}(a^\dagger a)^2\sigma_z + \hbar u_t x. \quad (18)$$

The last second term in Eq. (18) may induce nonlinear dynamics to the harmonic oscillator. However, $(g/\Delta_{qo})^2$ times in magnitude smaller compared with the third term in Eq. (18); it is too small to be observed in the large-detuning regime $g \ll \Delta_{qo}$. Thus, the high-order terms have been neglected in the following discussions.

The decay of the harmonic oscillator is detected by a homodyne measurement. Thus, the evolution of the qubit-oscillator system is conditioned on the measurement output of the homodyne detection, which can be described by the stochastic master equation (1) by replacing the system Hamiltonian H with $H_{\rm eff}$ given in Eq. (17). The output signal of the homodyne detection is integrated to obtain a new output signal $Y_t = \int_0^t dy/t$, which is further fed into a nonlinear controller to produce the control signal u_t given in Eq. (5). As presented in Sec. II, such a simple third-order nonlinear feedback control induces a static bifurcation that can be used to enhance the measurement strength for the qubit readout.

Different from the open-loop control that is predetermined by the designer without any information extraction, the

proposed feedback control u_t is automatically adjusted according to the state of the qubit in real time so that different controls generate different state trajectories and thus different output signals. This makes it possible to identify the state of the qubit by amplifying the difference between the output signals by the designed control. This feature of feedback control has been reported in the literature to enhance the measurement intensity by linear amplification (see, e.g., Ref. [35]), which can be done more efficiently via nonlinear amplification induced by the proposed quantum feedback control.

Let us assume that the qubit-oscillator system is initially in a separable state

$$\rho(0) = \rho_q(0) \otimes |\psi_0(0)\rangle\langle\psi_0(0)|,$$

where

$$\rho_q(0) = \sum_{i,j=g,e} \rho_{ij}(0)|i\rangle\langle j|$$

is the initial state of the qubit with ground state $|g\rangle$ and excited state $|e\rangle$ and $|\psi_0(0)\rangle$ is a Gaussian state of the harmonic oscillator with the first- and second-order quadratures given in Eq. (7). Then the stationary state of the qubit-oscillator system in the long-time limit can be expressed as [36]

$$\rho^{\infty} = \sum_{i,j=g,e} \rho_{ij}^{\infty} |i\rangle\langle j| \otimes \left|\alpha_i^{\infty}\right\rangle\left\langle\alpha_j^{\infty}\right|, \tag{19}$$

where both $|\alpha_e^{\infty}\rangle$ and $|\alpha_g^{\infty}\rangle$ are coherent states. Let

$$\alpha_{g,e}^{\infty} = \frac{1}{\sqrt{2}}\left(x_{g,e}^{\infty} + i p_{g,e}^{\infty}\right),$$

then $(x_g^{\infty}, p_g^{\infty})^T$ and $(x_e^{\infty}, p_e^{\infty})^T$ are respectively the stationary states of the equations

$$\begin{aligned} \dot{x}_{g,e} &= -\frac{\gamma}{2} x_{g,e} + (\Delta_{od} \mp \chi)\, p_{g,e}, \\ \dot{p}_{g,e} &= -\frac{\gamma}{2} p_{g,e} - (\Delta_{od} \mp \chi - k_1)\, x_{g,e} - k_3 x_{g,e}^3 + k_0. \end{aligned} \tag{20}$$

The coefficients ρ_{ij}^{∞} in Eq. (19) are given by

$$\rho_{gg}^{\infty} = \rho_{gg}(0), \quad \rho_{ee}^{\infty} = \rho_{ee}(0), \quad \rho_{ge}^{\infty} = \rho_{eg}^{\infty} = 0.$$

As analyzed in the last paragraph of Sec. II, the harmonic oscillator can be looked as a semiclassical pseudo-nonlinear system driven by an outer classical feedback control circuit (see the simplified version of the feedback control circuit in Fig. 3). The interaction between such a pseudo-nonlinear system and the qubit brings two aspects of effects. On the one hand, for the qubit, this interaction brings additional decoherence. In fact, it can be found that there exists a measurement-induced dephasing factor for the reduced states of the qubit for which the damping rate can be approximately estimated in the long-time limit as (see the analysis in Appendix B)

$$\Gamma = \chi\left(x_e^{\infty} p_g^{\infty} - p_e^{\infty} x_g^{\infty}\right). \tag{21}$$

On the other hand, this interaction leads to additional frequency shift for the harmonic oscillator depending on the state of the qubit. Therefore, it is possible to dispersively read out the states of the qubit under appropriate conditions.

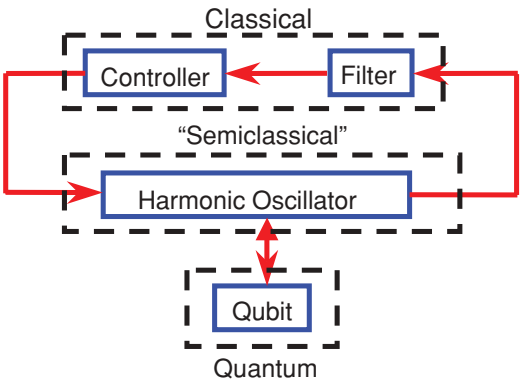

FIG. 3. (Color online) Simplified version for the feedback-control circuit of the coupled qubit-oscillator system. The qubit is coupled to the harmonic oscillator, which is driven by a feedback-control circuit composed of a filter and a controller. The nonlinear feedback control coming from the control circuit leads to semiclassical nonlinear dynamics of the harmonic oscillator. The static bifurcation induced by such nonlinear dynamics can be used to amplify small signals and thus measure the states of the qubit.

B. Bifurcation-induced quantum measurement

The equations of the harmonic oscillator corresponding to the ground and excited states of the qubit given in Eq. (20) have the same form as in Eq. (13) with two different angular frequencies $\omega = \Delta_{od} - \chi$ and $\omega = \Delta_{od} + \chi$. As analyzed in Sec. II, a static pitchfork bifurcation occurs at a critical angular frequency:

$$\omega^* = \tfrac{1}{2}\left(k_1 - \sqrt{k_1^2 - \gamma^2}\right).$$

When $\omega < \omega^*$, the system given by Eq. (13) possesses only one stable equilibrium, which becomes unstable when $\omega > \omega^*$ and, in the meanwhile, two other stable equilibria appear.

Therefore, by tuning the angular frequency ω_d of the driving field near the bifurcation point, the static bifurcation introduced by the proposed feedback control can induce a transition from weak to strong measurements for the qubit readout. Actually, if

$$\omega_d = \omega_o - \omega^* + 2\chi, \tag{22}$$

both effective angular frequencies $\omega_g = \omega^* - 3\chi$ and $\omega_e = \omega^* - \chi$ corresponding to the two eigenstates of the qubit are lower than ω^*. Then, in the long-time limit, for example, when $t \gg 1/\gamma$, the measurement outputs corresponding to the two eigenstates of the qubit are

$$Y_{g,e}(t) \to x_{g,e}^{\infty} = k_0 \frac{\omega_{g,e}}{\omega_{g,e}^2 - k_1\omega_{g,e} + \gamma^2/4}, \tag{23}$$

respectively [see Eq. (9) and the analysis in Appendix A]. If k_0 is small enough that

$$k_0 \ll \left|\frac{\chi^2 - 2\chi\omega^* + k_1\chi}{\omega^* - \chi}\right|, \tag{24}$$

both $Y_g(t)$ and $Y_e(t)$ are so close to zero that they are almost indistinguishable. When $t \gg 1/\gamma$, we have

$$x_{g,e} \to x_{g,e}^{\infty} = \frac{k_0\omega_{g,e}}{\omega_{g,e}^2 - k_1\omega_{g,e} + \gamma^2/4},$$

$$p_{g,e} \to p_{g,e}^{\infty} = \frac{\gamma}{2\omega_{g,e}} x_{g,e}^{\infty};$$

then we can calculate the measurement-induce dephasing rate Γ_{weak} from Eq. (21):

$$\begin{aligned}\Gamma_{\text{weak}} &= \chi\left(x_e^{\infty} p_g^{\infty} - p_e^{\infty} x_g^{\infty}\right) \\ &= \frac{\gamma k_0^2 \chi^2}{\left[\omega_g^2 - k_1\omega_g + \frac{\gamma^2}{4}\right]\left[\omega_e^2 - k_1\omega_e + \frac{\gamma^2}{4}\right]}.\end{aligned} \tag{25}$$

The tiny separation between $Y_g(t)$ and $Y_e(t)$ can be amplified by switching the angular frequency of the driving field from $\omega_d = \omega_o - \omega^* + 2\chi$ to $\tilde{\omega}_d = \omega_o - \omega^*$. Under this condition, the two effective angular frequencies $\tilde{\omega}_g = \omega^* - \chi$ and $\tilde{\omega}_e = \omega^* + \chi$ are lower and higher than the bifurcation angular frequency ω^*, respectively. When $t \gg 1/\gamma$, the corresponding stationary measurement outputs are

$$\begin{aligned}Y_g(t) \to \tilde{x}_g^{\infty} &= k_0 \frac{\tilde{\omega}_g}{\tilde{\omega}_g^2 - k_1\tilde{\omega}_g + \gamma^2/4}, \\ Y_e(t) \to \tilde{x}_e^{\infty} &= \sqrt{\frac{-\tilde{\omega}_e^2 + k_1\tilde{\omega}_e - \gamma^2/4}{k_3\tilde{\omega}_e}}.\end{aligned} \tag{26}$$

By setting

$$k_3 \ll \left|\frac{\chi^2 + 2\chi\omega^* - k_1\chi}{\omega^* + \chi}\right|, \tag{27}$$

we have

$$\left|\tilde{x}_e^{\infty} - \tilde{x}_g^{\infty}\right| \gg \left|x_e^{\infty} - x_g^{\infty}\right|.$$

The preceding result means that the difference between the two output signals corresponding to the two eigenstates of the qubit is amplified by the proposed nonlinear feedback control. When $t \gg 1/\gamma$, it can be calculated that

$$\begin{aligned}x_g \to \tilde{x}_g^{\infty} &= k_0 \frac{\tilde{\omega}_g}{\tilde{\omega}_g^2 - k_1\tilde{\omega}_g + \gamma^2/4}, \\ x_e \to \tilde{x}_e^{\infty} &= \sqrt{\frac{-\tilde{\omega}_e^2 + k_1\tilde{\omega}_e - \gamma^2/4}{k_3\tilde{\omega}_e}}, \\ p_g \to \tilde{p}_g^{\infty} &= \frac{\gamma}{2\tilde{\omega}_g}\tilde{x}_g^{\infty}, \\ p_e \to \tilde{p}_e^{\infty} &= \frac{\gamma}{2\tilde{\omega}_e}\tilde{x}_e^{\infty}.\end{aligned}$$

Then, we can obtain the measurement-induced dephasing rate Γ_{strong} from Eq. (21) as

$$\begin{aligned}\Gamma_{\text{strong}} &= \chi\left(\tilde{x}_e^{\infty}\tilde{p}_g^{\infty} - \tilde{p}_e^{\infty}\tilde{x}_g^{\infty}\right) \\ &= \frac{k_0\gamma\chi^2}{\sqrt{k_3\tilde{\omega}_e^3}} \cdot \frac{\sqrt{-\tilde{\omega}_e^2 + k_1\tilde{\omega}_e - \gamma^2/4}}{\tilde{\omega}_g^2 - k_1\tilde{\omega}_g + \gamma^2/4}.\end{aligned} \tag{28}$$

It can be noticed that Γ_{strong} is far greater than Γ_{weak} when k_0 and k_3 are sufficiently small to satisfy Eqs. (24) and (27).

IV. APPLICATIONS

A. Atom-optical systems

Consider a coupled atom-cavity system in which a two-level C_s atom is dispersively coupled to a single-mode field in an optical cavity [37] (see Fig. 4). The probe light transmitted through the optical cavity is detected by a homodyne measurement. Then the output photon current is fed into a control circuit composed of an integral filter and a controller to generate a control signal, which is further fed back to control the probe light by a modulator.

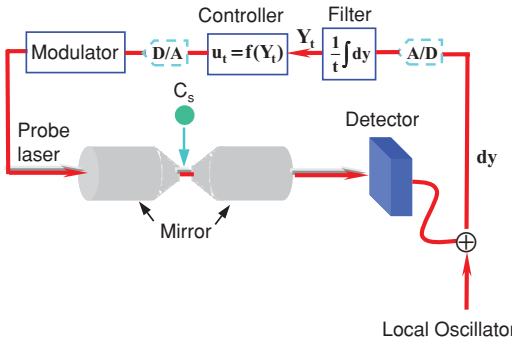

FIG. 4. (Color online) Schematic diagram of the atom-optical system under feedback control. A two-level C_s atom is coupled to a single-mode quantum field in the optical cavity, whose output field is detected by a homodyne measurement. The output signal of the homodyne measurement is fed into an electric control circuit to generate the desired control signal, which is further fed back to modulate the probe laser fed into the optical cavity. The output signal of the homodyne detection may also be converted into a digital signal via an analog/digital (A/D) signal convertor, and thus the control signal can be generated by a digital signal processor, which is further converted into an electric signal via a digital/analog (D/A) signal convertor and fed back.

We choose the following experimentally accessible parameters (see, e.g., Refs. [37–39]):

$$\begin{aligned}\Delta_{qo}/2\pi &= 35 \text{ MHz}, \\ g/2\pi &= 8 \text{ MHz}, \\ \gamma/2\pi &= 1.4 \text{ MHz},\end{aligned}$$

where $\Delta_{qo} = \omega_q - \omega_o$ is the detuning between the frequency ω_q of the two-level atom and the frequency ω_o of the single-mode field in the optical cavity; g is the coupling constant between the two-level atom and the optical cavity; and γ is the damping rate of the optical cavity. The control parameters k_0, k_1, and k_3 are chosen to be

$$\begin{aligned}k_0/2\pi &= 1 \text{ MHz}, \\ k_1/2\pi &= 6 \text{ MHz}, \\ k_3/2\pi &= 1 \text{ MHz}.\end{aligned}$$

We first tune the detuning $\Delta_{od} = \omega_o - \omega_d$ between the frequency ω_o of the optical cavity and the frequency ω_d of the driving field such that

$$\Delta_{od}/2\pi = -3.57 \text{ MHz}.$$

In this case, the long-time limits of the measurement outputs Y_g and Y_e corresponding to the ground and excited states $|g\rangle$ and $|e\rangle$ of the two-level atom are both close to zero and thus almost indistinguishable [see Fig. 5(a)]. This corresponds to the weak measurement case.If we tune the detuning frequency

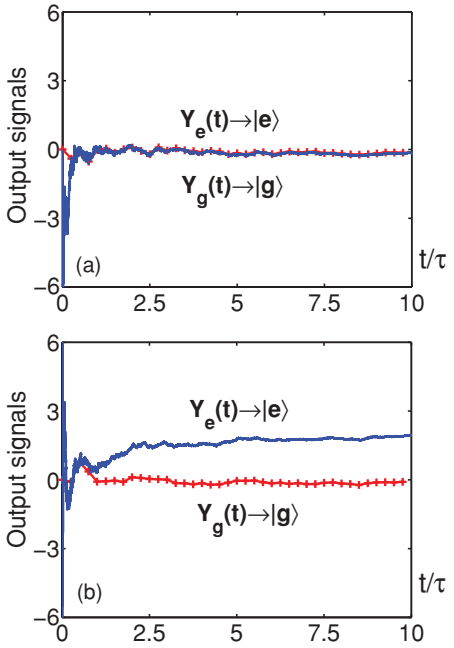

FIG. 5. (Color online) Measurement outputs of the atom-cavity system under feedback control. (a) $\Delta_{od}/2\pi = -3.57$ MHz (weak measurement case): The two output signals $Y_g(t)$ (red curve with plus signs) and $Y_e(t)$ (blue solid curve) corresponding to the two eigenstates $|g\rangle$ and $|e\rangle$ of the two-level atom are almost indistinguishable. (b) $\Delta_{od}/2\pi = 0.083$ MHz (strong measurement case): The two output signals $Y_g(t)$ (red curve with plus signs) and $Y_e(t)$ (blue solid curve) are separated in the long-time limit. The parameter $\tau = 0.16$ μs is the normalization time scale.

Δ_{od} such that

$$\Delta_{od}/2\pi = 0.083 \text{ MHz},$$

the two branches of outputs corresponding to $|g\rangle$ and $|e\rangle$ are separated in the long-time limit, which corresponds to the strong measurement case [see Fig. 5(b)].

B. Superconducting circuits

The second example considers the superconducting circuit shown in Fig. 6, in which a transmission line resonator is capacitively coupled to a Cooper pair box (charge qubit).

Let us now discuss experimental feasibility via the numerical simulation using the experimentally accessible parameters. According to the current experiments (see, e.g., Ref. [40]), the qubit frequency ω_q, the frequency ω_o, and the decay rate γ of the transmission line resonator, as well as the coupling constant g between the qubit and the transmission line resonator, can be chosen as

$$\begin{aligned} &\omega_q/2\pi = 5.1 \text{ GHz}, \quad \omega_o/2\pi = 5 \text{ GHz}, \\ &\gamma/2\pi = 100 \text{ MHz}, \quad g/2\pi = 20 \text{ MHz}. \end{aligned} \tag{29}$$

With the conditions given in Eqs. (24) and (27), we further assume that the parameters k_0, k_1, and k_3 are

$$\begin{aligned} &k_0/2\pi = 20 \text{ MHz}, \\ &k_1/2\pi = 200 \text{ MHz}, \\ &k_3/2\pi = 2 \text{ or } 10 \text{ MHz}. \end{aligned} \tag{30}$$

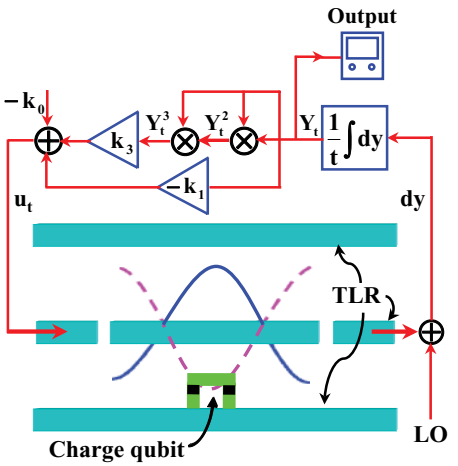

FIG. 6. (Color online) Schematic diagram of the superconducting circuit under feedback control. A charge qubit is capacitively coupled to a transmission line resonator (TLR), whose output field is detected by a homodyne measurement ("LO" denotes a local oscillator). The output signal of the homodyne measurement is fed into an electric control circuit to generate the desired control signal, which is further used to drive the electric field in the transmission line resonator.

The frequency $\omega_d/2\pi$ of the driving field is initially chosen to be 4.995 GHz. At the time $t^*/\tau = 100$, that is, $t^* = 50$ ns, the frequency $\omega_d/2\pi$ of the driving field is switched from 4.995 GHz to 4.987 GHz, where $\tau = 0.5$ ns is a normalization time scale. Simulation results in Fig. 7 show that, at time t^*, the difference between the two output signals $Y_g(t)$ and $Y_e(t)$,

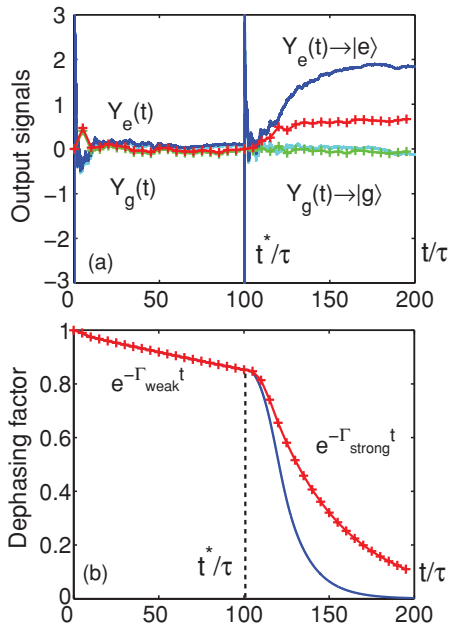

FIG. 7. (Color online) Bifurcation-induced transition from a weak measurement to a strong measurement with (a) the two output signals $Y_g(t)$ and $Y_e(t)$ corresponding to the two eigenstates $|g\rangle$ and $|e\rangle$ of the charge qubit and (b) the measurement-induced dephasing factor. The parameter $\tau = 0.5$ ns is the normalization time scale. The solid curves represent the trajectories with a nonlinear coefficient $k_3/2\pi = 2$ MHz, while the solid curves with plus signs represent the trajectories with $k_3/2\pi = 10$ MHz.

that is, the measurement sensitivity, suddenly jumps. The measurement-induced dephasing rate also suddenly jumps from Γ_{weak} to Γ_{strong}. In fact, it can be calculated from Eqs. (25) and (28) that $\Gamma_{\text{weak}}/2\pi \approx 0.36$ MHz and $\Gamma_{\text{strong}}/2\pi \approx 10.22$ MHz (or 4.57 MHz) when $k_3/2\pi = 2$ MHz (or 10 MHz). This indicates that the static bifurcation introduced by our proposal induces a transition from weak to strong measurements at time t^*. Moreover, as shown in Eq. (26) and the simulation results in Fig. 7, the decrease of the nonlinear coefficient k_3 makes the measurement more sensitive, but accelerates the dephasing of the qubit. Such a tradeoff between measurement sensitivity and measurement-induced dephasing effects is a natural consequence of the conflict between information extraction and measurement-induced disturbance, which is inherent for quantum measurement.

V. CONCLUSION

In summary, we present a method to induce semiclassical nonlinear dynamics in a damped harmonic oscillator via quantum feedback control. The nonlinear feedback control induces a static bifurcation, which can be used to amplify the small frequency shift of the harmonic oscillator for the qubit readout. Theoretical analysis and numerical simulations show an evident transition from weak to strong measurements near the bifurcation point. Our proposal works as well as the bifurcation readout proposal by a nonlinear amplifier, for example, a rf-driven Josephson junction. Additionally, we can tune the information extraction rate to balance between information extraction and measurement-induced disturbance in the nonlinear readout regime. Using the atom-optical systems and circuit QED systems as examples, we show how to apply our proposal to experimental systems.

We emphasize that the proposed cavity-assistant nonlinear amplification strategy can also be applied to the qubit readouts in other experimental implementations, such as quantum dot-cavity systems. This generalized result is important in that the proposed measurement method might be more efficient, because the nonlinear amplification device, like the rf-driven Josephson junctions in superconducting circuits, may not be achievable.

We hope our study can also be extended to quantum demolition measurements, for example, the detection of momentum or position of a nanomechanical resonator, for which the measurement-induced back-action effects on the quantity being measured cannot be neglected.

ACKNOWLEDGMENTS

We acknowledge financial support from the National Natural Science Foundation of China under Grants No. 60704017, No. 10975080, No. 60904034, No. 60836001, and No. 60635040. T. J. Tarn also acknowledges partial support from the US Army Research Office under Grant No. W911NF-04-1-0386.

APPENDIX A: DYNAMICS OF THE CONTROLLED HARMONIC OSCILLATOR

From the stochastic master equation (1) and the measurement output equation (2) given in Sec. II, we can obtain the following non-Markovian stochastic integrodifferential equations for $\langle x\rangle$ and $\langle p\rangle$:

$$\begin{aligned} d\langle x\rangle &= -\frac{\gamma}{2}\langle x\rangle dt + \omega\langle p\rangle dt + \sqrt{2\eta\gamma}\left(V_x - \frac{1}{2}\right), \\ d\langle p\rangle &= -\omega\langle x\rangle dt - \frac{\gamma}{2}\langle p\rangle dt + k_0 dt + \sqrt{2\eta\gamma}C_{xp}dW \\ &\quad + k_1\frac{1}{t}\int_0^t\left(\langle x\rangle dt + \frac{1}{\sqrt{2\eta\gamma}}dW\right) \\ &\quad - k_3\left[\frac{1}{t}\int_0^t\left(\langle x\rangle dt + \frac{1}{\sqrt{2\eta\gamma}}dW\right)\right]^3, \end{aligned} \tag{A1}$$

which are equivalent to stochastic Markovian equations by introducing a new variable Y_t:

$$\begin{aligned} d\langle x\rangle &= -\frac{\gamma}{2}\langle x\rangle dt + \omega\langle p\rangle dt + \sqrt{2\eta\gamma}\left(V_x - \frac{1}{2}\right)dW, \\ d\langle p\rangle &= -\omega\langle x\rangle dt - \frac{\gamma}{2}\langle p\rangle dt + \left(k_1 Y_t - k_3 Y_t^3 + k_0\right)dt \\ &\quad + \sqrt{2\eta\gamma}C_{xp}dW, \\ dY_t &= -\frac{1}{t}(Y_t - \langle x\rangle)dt - \frac{1}{t\sqrt{2\eta\gamma}}dW, \end{aligned} \tag{A2}$$

where

$$V_x = \langle x^2\rangle - \langle x\rangle^2, \quad V_p = \langle p^2\rangle - \langle p\rangle^2$$

are the variances of the position x and momentum p and

$$C_{xp} = \left\langle\frac{xp + px}{2}\right\rangle - \langle x\rangle\langle p\rangle$$

is the symmetric covariance of x and p.

Taking the average of the preceding equations, we have

$$\begin{aligned} \dot{\bar{x}} &= -\frac{\gamma}{2}\bar{x} + \omega\bar{p}, \\ \dot{\bar{p}} &= -\omega\bar{x} - \frac{\gamma}{2}\bar{p} + k_1\bar{Y}_t - k_3\bar{Y}_t^3 + k_0, \\ \dot{\bar{Y}}_t &= -\frac{1}{t}(\bar{Y}_t - \bar{x}), \end{aligned} \tag{A3}$$

where $\bar{x} = E(\langle x\rangle)$, $\bar{p} = E(\langle p\rangle)$, and $\bar{Y}_t = E(Y_t)$. Here we neglect the high-order correlation of Y_t induced by the classical noise dW which is reasonable when the evolution time is sufficiently long.

When $\omega < \omega^*$, we have

$$\begin{aligned} x_0^\infty &= k_0\frac{\omega}{\omega^2 - k_1\omega + \gamma^2/4} > 0, \\ p_0^\infty &= k_0\frac{\gamma/2}{\omega^2 - k_1\omega + \gamma^2/4} > 0. \end{aligned} \tag{A4}$$

Then, since we start from the initial state $(0,0,0)^T$, it can be verified from Eq. (A3) that

$$0 \leqslant \bar{x} \leqslant x_0^\infty, \quad 0 \leqslant \bar{p} \leqslant p_0^\infty, \quad 0 \leqslant \bar{Y}_t \leqslant x_0^\infty.$$

Thus, from the last equation in Eq. (A3), we have $\dot{\bar{Y}}_t \to 0$, that is, $\exists Y^\infty$, such that $\bar{Y}_t \to Y^\infty$ when $t \to \infty$. Substituting Y^∞ into the first two equations of Eq. (A3), we have

$$\begin{pmatrix}\dot{\bar{x}}\\ \dot{\bar{p}}\end{pmatrix} = \begin{pmatrix}-\frac{\gamma}{2} & \omega\\ -\omega & -\frac{\gamma}{2}\end{pmatrix}\begin{pmatrix}\bar{x}\\ \bar{p}\end{pmatrix} + \begin{pmatrix}0\\ k_1 Y^\infty - k_3 Y^{\infty 3} + k_0\end{pmatrix}.$$

Since the matrix

$$\begin{pmatrix} -\frac{\gamma}{2} & \omega \\ -\omega & -\frac{\gamma}{2} \end{pmatrix} < 0,$$

we know that there exists $(x^\infty, p^\infty)^T$ such that

$$\begin{pmatrix} \bar{x}(t) \\ \bar{p}(t) \end{pmatrix} \to \begin{pmatrix} x^\infty \\ p^\infty \end{pmatrix},$$

when $t \to \infty$.

Next we show that $Y^\infty = x^\infty$. Note that

$$\bar{Y}_t = E(Y_t) = \frac{1}{t}\int_0^t \bar{x}(\tau)\, d\tau,$$

so we know that $\forall\, \epsilon > 0, \exists\, T_\sigma$, such that $\forall\, t > T_\sigma, |\bar{x} - x^\infty| < \epsilon/2$. Let

$$\Delta(T_\sigma) = \max_{[0,T_\sigma]} |\bar{x} - x^\infty|$$

and

$$T_Y = \max\{T_\sigma, 2\epsilon^{-1} T_\sigma \Delta(T_\sigma)\}.$$

Then $\forall\, t > T_Y$, so we have

$$\begin{aligned} |\bar{Y}_t - x^\infty| &< \frac{1}{t}\int_0^{T_\sigma} |\bar{x}(s) - x^\infty| ds + \frac{1}{t}\int_{T_\sigma}^t |\bar{x}(s) - x^\infty| ds \\ &< \frac{\epsilon}{2T_\sigma \Delta(T_\sigma)} \cdot T_\sigma \Delta(T_\sigma) + \frac{\epsilon}{2} = \epsilon, \end{aligned}$$

which means that $Y^\infty = x^\infty$.

In order to solve $(x^\infty, p^\infty)^T$, we let $\dot{\bar{x}} = 0$, $\dot{\bar{p}} = 0$ to obtain the algebraic equations

$$\begin{aligned} 0 &= -\frac{\gamma}{2} x^\infty + \omega p^\infty, \\ 0 &= -\omega x^\infty - \frac{\gamma}{2} p^\infty + k_1 x^\infty - k_3 (x^\infty)^3 + k_0. \end{aligned}$$

Although three equilibria can be solved in this case, only one equilibrium $(x_0^\infty, p_0^\infty)^T$ is stable when $\omega < \omega^*$, where x_0^∞, p_0^∞ are given by Eq. (A4). Thus, if $\omega < \omega^*$, we have

$$\begin{aligned} E(\langle x \rangle) = \bar{x} &\to x_0^\infty, \\ E(\langle p \rangle) = \bar{p} &\to p_0^\infty, \\ E(Y_t) = \bar{Y}_t &\to Y_0^\infty = x_0^\infty, \end{aligned} \tag{A5}$$

when $t \to \infty$.

Furthermore, it can be calculated that the equations of higher-order quadratures are independent of the control u_t. Thus, the evolutions of higher-order quadratures are like those of a linear harmonic oscillator. Since we start from a Gaussian state, the state given by Eq. (1) remains a Gaussian state, and thus we only need to calculate the variances V_x, V_p and the symmetric covariance C_{xp}. From Eq. (1), we can obtain that

$$\begin{aligned} \dot{V}_x &= -\gamma V_x + 2\omega C_{xp} + \frac{\gamma}{2} - 2\eta\gamma \left(V_x - \frac{1}{2}\right)^2, \\ \dot{V}_p &= -\gamma V_p - 2\omega C_{xp} + \frac{\gamma}{2} - 2\eta\gamma C_{xp}^2, \\ \dot{C}_{xp} &= -\gamma C_{xp} + \omega V_p - \omega V_x - 2\eta\gamma \left(V_x - \frac{1}{2}\right) C_{xp}, \end{aligned} \tag{A6}$$

from which it can be verified that

$$\begin{aligned} V_x &\to V_x^\infty = 1/2, \\ V_p &\to V_p^\infty = 1/2, \\ C_{xp} &\to C_{xp}^\infty = 0, \end{aligned} \tag{A7}$$

when $t \to \infty$. From Eqs. (A5) and (A7), we know that the state of the controlled harmonic oscillator tends to a stationary coherent state $|\alpha_0^\infty\rangle$ given by Eq. (8) when $\omega < \omega^*$.

With the same discussions, it can be verified that there exist two stable equilibria for Eq. (A3) when $\omega > \omega^*$, which can be expressed as

$$\begin{pmatrix} x_{1,2}^\infty \\ p_{1,2}^\infty \\ Y_{1,2}^\infty \end{pmatrix} = \pm\sqrt{\frac{-\omega^2 + k_1\omega - \gamma^2/4}{k_3\omega}} \begin{pmatrix} 1 \\ 2\omega/\gamma \\ 1 \end{pmatrix}, \tag{A8}$$

and Eq. (A7) can also be obtained in this case. It means that the state of the controlled harmonic oscillator tends to $|\alpha_1^\infty\rangle$ or $|\alpha_2^\infty\rangle$ when $\omega > \omega^*$.

APPENDIX B: APPROXIMATE ESTIMATE OF THE MEASUREMENT-INDUCED DEPHASING RATE

With the same analysis as in Appendix A of Ref. [41], the state of the qubit-oscillator system can be expressed as

$$\rho(t) = \sum_{i,j=g,e} \rho_{ij}(t) |i\rangle\langle j| \otimes |\psi_i(t)\rangle\langle\psi_j(t)|,$$

where $|\psi_e\rangle$ and $|\psi_g\rangle$ are Gaussian states with first- and second-order quadratures in the phase space as

$$\begin{aligned} \langle x \rangle_{g,e} &= x_{g,e}, \quad \langle p \rangle_{g,e} = p_{g,e}, \\ \langle x^2 \rangle_{g,e} - \langle x \rangle_{g,e}^2 &= V_{g,e}^x, \\ \langle p^2 \rangle_{g,e} - \langle p \rangle_{g,e}^2 &= V_{g,e}^p, \\ \left\langle \frac{xp + px}{2} \right\rangle_{g,e} - \langle x \rangle_{g,e} \langle p \rangle_{g,e} &= C_{g,e}^{xp}. \end{aligned}$$

The first-order quadratures $x_{g,e}$, $p_{g,e}$ satisfy the equations

$$\begin{aligned} d\, x_{g,e} &= -\frac{\gamma}{2} x_{g,e} dt + (\Delta_{od} \mp \chi) p_{g,e}\, dt \\ &\quad + \sqrt{2\eta\gamma} \left(V_{g,e}^x - \frac{1}{2}\right) dW, \\ d\, p_{g,e} &= -(\Delta_{od} \mp \chi) x_{g,e} dt - \frac{\gamma}{2} p_{g,e}\, dt \\ &\quad + \left(k_1 Y_{g,e} - k_3 Y_{g,e}^3 + k_0\right) dt + \sqrt{2\eta\gamma} C_{g,e}^{ep}\, dW, \\ d\, Y_{g,e} &= -\frac{1}{t}(Y_{g,e} - x_{g,e})\, dt - \frac{1}{t\sqrt{2\eta\gamma}}\, dW, \end{aligned}$$

and the second-order quadratures $V_{g,e}^x$, $V_{g,e}^p$, $C_{g,e}^{xp}$ satisfy the equations

$$\begin{aligned} \dot{V}_{g,e}^x &= -\gamma V_{g,e}^x + 2(\Delta_{od} \mp \chi) C_{g,e}^{xp} \\ &\quad + \frac{\gamma}{2} - 2\eta\gamma \left(V_{g,e}^x - \frac{1}{2}\right)^2, \\ \dot{V}_{g,e}^p &= -\gamma V_{g,e}^p - 2(\Delta_{od} \mp \chi) C_{g,e}^{xp} + \frac{\gamma}{2} - 2\eta\gamma \left(C_{g,e}^{xp}\right)^2, \end{aligned}$$

$$\dot{C}^{xp}_{g,e} = -\gamma C^{xp}_{g,e} + (\Delta_{od} \mp \chi)V^{p}_{g,e} - (\Delta_{od} \mp \chi)V^{x}_{g,e} - 2\eta\gamma\left(V^{x}_{g,e} - \frac{1}{2}\right)C^{xp}_{g,e}.$$

Here, as an approximate estimation, we omit the higher-order disturbance induced by $V^{x}_{g,e}$, $V^{p}_{g,e}$, and $C^{xp}_{g,e}$; then the coefficients $\rho_{ij}(t)$ are given by (see, e.g., Ref. [36])

$$\rho_{gg}(t) = \rho_{gg}(0), \quad \rho_{ee}(t) = \rho_{ee}(0), \quad \rho_{ge}(t) = \rho^{*}_{eg}(t),$$
$$\rho_{eg}(t) = \frac{\exp[-(\gamma_2 t + \Sigma(t)) - i(\omega_q t + \Theta(t))]}{\langle\psi_g(t)|\psi_e(t)\rangle}\rho_{eg}(0),$$

where γ_2 is the dephasing rate of the qubit without measurement, and $\Sigma(t)$ and $\Theta(t)$ can be expressed as

$$\Sigma(t) = \chi\int_0^t [x_e(s)p_g(s) - p_e(s)x_g(s)]\,ds, \tag{B1}$$

$$\Theta(t) = \chi\int_0^t [x_e(s)x_g(s) + p_e(s)p_g(s)]\,ds. \tag{B2}$$

By tracing out the degrees of freedom of the harmonic oscillator, it can be shown that there exists a measurement-induced dephasing factor $\exp[-\Sigma(t)]$.

As is proved in Appendix A, we have $x_{g,e} \to x^{\infty}_{g,e}$, $p_{g,e} \to p^{\infty}_{g,e}$ in the long-time limit. Thus, for any $s > \bar{t} \gg 1/\gamma$, it can be approximately estimated as $x_{g,e}(s) \approx x^{\infty}_{g,e}$, $p_{g,e}(s) \approx p^{\infty}_{g,e}$. Then the measurement-induced dephasing after $\bar{t}$ can be approximately calculated as

$$\exp\left\{\chi\int_{\bar{t}}^{t}[x_e(s)p_g(s) - p_e(s)x_g(s)]\,ds\right\} \approx \exp\left\{\left[\chi\left(x^{\infty}_{e}p^{\infty}_{g} - p^{\infty}_{e}x^{\infty}_{g}\right)\right](t-\bar{t})\right\},$$

which leads to Eq. (21).

[1] H. M. Wiseman and G. J. Milburn, *Quantum Measurement and Control* (Cambridge University Press, Cambridge, UK, 2009).

[2] D. D'Alessandro, *Introduction to Quantum Control and Dynamics* (Chapman & Hall, Boca Raton, FL, 2007).

[3] H. Mabuchi and N. Khaneja, Int. J. Robust Nonlinear Control **15**, 647 (2005).

[4] D. Y. Dong and I. R. Petersen, e-print arXiv:0910.2350v1 [quant-ph].

[5] N. Ganesan and T. J. Tarn, Phys. Rev. A **75**, 032323 (2007); R. B. Wu, T. J. Tarn, and C. W. Li, *ibid.* **73**, 012719 (2006); D. Y. Dong, C. B. Zhang, H. Rabitz, A. Pechen, and T. J. Tarn, J. Chem. Phys. **129**, 154103 (2008); W. Cui, Z. R. Xi, and Y. Pan, Phys. Rev. A **77**, 032117 (2008); J. Phys. A **42**, 025303 (2009); M. Zhang, H. Y. Dai, Z. R. Xi, H. W. Xie, and D. W. Hu, Phys. Rev. A **76**, 042335 (2007).

[6] J. Zhang, C. W. Li, R. B. Wu, T. J. Tarn, and X. S. Liu, J. Phys. A **38**, 6587 (2005); J. Zhang, R. B. Wu, C. W. Li, T. J. Tarn, and J. W. Wu, Phys. Rev. A **75**, 022324 (2007); J. Zhang, Y.-X. Liu, C. W. Li, T. J. Tarn, and F. Nori, *ibid.* **79**, 052308 (2009); J. Zhang, R. B. Wu, C. W. Li, and T. J. Tarn, IEEE Trans. Autom. Control **55**, 619 (2010).

[7] V. P. Belavkin, J. Multivariate Anal. **42**, 171 (1992); Commun. Math. Phys. **146**, 611 (1992); Theory Probab. Appl. **38**, 573 (1993).

[8] H. M. Wiseman and G. J. Milburn, Phys. Rev. Lett. **70**, 548 (1993); Phys. Rev. A **47**, 642 (1993).

[9] A. C. Doherty, S. Habib, K. Jacobs, H. Mabuchi, and S. M. Tan, Phys. Rev. A **62**, 012105 (2000).

[10] M. R. James, H. I. Nurdin, and I. R. Petersen, IEEE Trans. Autom. Control **53**, 1787 (2008); J. E. Gough, Phys. Rev. A **78**, 052311 (2008); N. Yamamoto, *ibid.* **74**, 032107 (2006).

[11] R. Ruskov and A. N. Korotkov, Phys. Rev. B **66**, 041401(R) (2002); L. Bouten, R. van Handel, and M. R. James, SIAM J. Control Optim. **46**, 2199 (2007); L. Bouten, M. Guta, and H. Maassen, J. Phys. A **37**, 3189 (2004).

[12] H. Mabuchi and A. C. Doherty, Science **298**, 1372 (2002).

[13] R. L. Cook, P. J. Martin, and J. M. Geremia, Nature (London) **446**, 774 (2007).

[14] G. G. Gillett, R. B. Dalton, B. P. Lanyon, M. P. Almeida, M. Barbieri, G. J. Pryde, J. L. O'Brien, K. J. Resch, S. D. Bartlett, and A. G. White, Phys. Rev. Lett. **104**, 080503 (2010).

[15] J. Q. You and F. Nori, Phys. Today **58**, 42 (2005); Y. Makhlin, G. Schön, and A. Shnirman, Rev. Mod. Phys. **73**, 357 (2001); J. Clarke and F. K. Wilhelm, Nature (London) **453**, 1031 (2008); A. A. Clerk, M. H. Devoret, S. M. Girvin, F. Marquardt, and R. J. Schoelkopf, Rev. Mod. Phys. **82**, 1155 (2010).

[16] R. van Handel, J. K. Stockton, and H. Mabuchi, IEEE Trans. Autom. Control **50**, 768 (2005); H. F. Hofmann, G. Mahler, and O. Hess, Phys. Rev. A **57**, 4877 (1998); J. Wang and H. M. Wiseman, *ibid.* **64**, 063810 (2001); X. S. Liu, W. Z. Liu, R. B. Wu, and G. L. Long, J. Opt. B **7**, 66 (2005); H. M. Wiseman, S. Mancini, and J. Wang, Phys. Rev. A **66**, 013807 (2002).

[17] S. Mancini and H. M. Wiseman, Phys. Rev. A **75**, 012330 (2007); C. Hill and J. Ralph, *ibid.* **77**, 014305 (2008); A. R. R. Carvalho and J. J. Hope, *ibid.* **76**, 010301(R) (2007); S. Mancini and J. Wang, Eur. Phys. J. D **32**, 257 (2005).

[18] L. K. Thomsen, S. Mancini, and H. M. Wiseman, Phys. Rev. A **65**, 061801(R) (2002); X. Wang, A. SøndbergSørensen, and K. Mølmer, *ibid.* **64**, 053815 (2001); X. G. Wang, A. Miranowicz, Y.-X. Liu, C. P. Sun, and F. Nori, *ibid.* **81**, 022106 (2010).

[19] P. Zhang, Y. D. Wang, and C. P. Sun, Phys. Rev. Lett. **95**, 097204 (2005); J. Q. You, Y. X. Liu, and F. Nori, *ibid.* **100**, 047001 (2008); M. Grajcar, S. Ashhab, J. R. Johansson, and F. Nori, Phys. Rev. B **78**, 035406 (2008); Y. D. Wang, Y. Li, F. Xue, C. Bruder, and K. Semba, *ibid.* **80**, 144508 (2009); F. Xue, Y. D. Wang, Y. X. Liu, and F. Nori, *ibid.* **76**, 205302 (2007); N. Lambert and F. Nori, *ibid.* **78**, 214302 (2008); S. H. Ouyang, J. Q. You, and F. Nori, *ibid.* **79**, 075304 (2009).

[20] R. Ruskov, K. Schwab, and A. N. Korotkov, Phys. Rev. B **71**, 235407 (2005).

[21] A. Hopkins, K. Jacobs, S. Habib, and K. C. Schwab, Phys. Rev. B **68**, 235328 (2003).

[22] J. Zhang, Y. X. Liu, and F. Nori, Phys. Rev. A **79**, 052102 (2009).

[23] K. Jähne, C. Genes, K. Hammerer, M. Wallquist, E. S. Polzik, and P. Zoller, Phys. Rev. A **79**, 063819 (2009); Ya. S. Greenberg, E. Il'ichev, and F. Nori, Phys. Rev. B **80**, 214423 (2009).

[24] M. P. Blencowe and E. Buks, Phys. Rev. B **76**, 014511 (2007); E. Buks and M. P. Blencowe, *ibid.* **74**, 174504 (2006); E. Buks, S. Zaitsev, E. Segev, B. Abdo, and M. P. Blencowe, Phys. Rev. E **76**, 026217 (2007).

[25] S. Etaki, M. Poot, I. Mahboob, K. Onomitsu, H. Yamaguchi, and H. S. J. van der Zant, Nat. Phys. **4**, 785 (2008).

[26] T. Bhattacharya, S. Habib, and K. Jacobs, Phys. Rev. Lett. **85**, 4852 (2000); S. Habib, K. Jacobs, and K. Shizume, *ibid.* **96**, 010403 (2006).

[27] M. A. Armen and H. Mabuchi, Phys. Rev. A **73**, 063801 (2006).

[28] I. Siddiqi, R. Vijay, F. Pierre, C. M. Wilson, M. Metcalfe, C. Rigetti, L. Frunzio, and M. H. Devoret, Phys. Rev. Lett. **93**, 207002 (2004); I. Siddiqi, R. Vijay, M. Metcalfe, E. Boaknin, L. Frunzio, R. J. Schoelkopf, and M. H. Devoret, Phys. Rev. B **73**, 054510 (2006).

[29] A. Lupascu, C. J. M. Verwijs, R. N. Schouten, C. J. P. M. Harmans, and J. E. Mooij, Phys. Rev. Lett. **93**, 177006 (2004); A. Lupascu, E. F. C. Driessen, L. Roschier, C. J. P. M. Harmans, and J. E. Mooij, *ibid.* **96**, 127003 (2006); A. Lupascu, S. Saito, T. Picot, P. C. de Groot, C. J. P. M. Harmans, and J. E. Mooij, Nat. Phys. **3**, 119 (2007).

[30] A. Isidori, *Nonlinear Control Systems* (Springer Verlag, London, 1995), 3rd ed.

[31] K. Jacobs and A. P. Lund, Phys. Rev. Lett. **99**, 020501 (2007).

[32] S. Ashhab, J. Q. You, and F. Nori, Phys. Rev. A **79**, 032317 (2009); New J. Phys. **11**, 083017 (2009); Phys. Scr. T **137**, 014005 (2009).

[33] J. K. Stockton, R. van Handel, and H. Mabuchi, Phys. Rev. A **70**, 022106 (2004).

[34] K. Petersen, *Ergodic Theory (Cambridge Studies in Advanced Mathematics)* (Cambridge University Press, Cambridge, UK, 1990).

[35] J. Combes, H. M. Wiseman, and K. Jacobs, Phys. Rev. Lett. **100**, 160503 (2008).

[36] J. Gambetta, A. Blais, M. Boissonneault, A. A. Houck, D. I. Schuster, and S. M. Girvin, Phys. Rev. A **77**, 012112 (2008); D. WahyuUtami and A. A. Clerk, *ibid.* **78**, 042323 (2008).

[37] C. J. Hood, T. W. Lynn, A. C. Doherty, A. S. Parkins, and H. J. Kimble, Science **287**, 1447 (2000).

[38] C. J. Hood, M. S. Chapman, T. W. Lynn, and H. J. Kimble, Phys. Rev. Lett. **80**, 4157 (1998).

[39] T. Puppe, I. Schuster, A. Grothe, A. Kubanek, K. Murr, P. W. H. Pinkse, and G. Rempe, Phys. Rev. Lett. **99**, 013002 (2007).

[40] A. Blais, R. S. Huang, A. Wallraff, S. M. Girvin, and R. J. Schoelkopf, Phys. Rev. A **69**, 062320 (2004); A. Wallraff, D. I. Schuster, A. Blais, L. Frunzio, R.-S. Huang, J. Majer, S. Kumar, S. M. Girvin, and R. J. Schoelkopf, Nature (London) **431**, 162 (2004).

[41] J. Gambetta, A. Blais, D. I. Schuster, A. Wallraff, L. Frunzio, J. Majer, M. H. Devoret, S. M. Girvin, and R. J. Schoelkopf, Phys. Rev. A **74**, 042318 (2006).